

Photoinduced Electron Transfer at Liquid/Liquid Interfaces. Part III. Photoelectrochemical Responses Involving Porphyrin Ion Pairs

David J. Fermín, H. Dung Duong, Zhifeng Ding, Pierre-François Brevet, and
Hubert H. Girault*

Contribution from the Laboratoire d'Electrochimie, Departement de Chimie, Ecole Polytechnique Fédérale de Lausanne, CH-1015 Lausanne, Switzerland

Received June 28, 1999

Abstract: The interfacial photoreactivity of water soluble porphyrin ion pairs was explored by photocurrent measurements at the water/1,2-dichloroethane interface. The anionic zinc meso-tetrakis(*p*-sulfonatophenyl)-porphyrin and cationic zinc tetrakis(*N*-methylpyridyl)porphyrin undergo spontaneous association in solution, leading to electrically neutral surface active heterodimer species. Heterogeneous quenching of the porphyrin ion pair was observed in the presence of the electron donor decamethylferrocene and the electron acceptor tetracyanoquinodimethane. No substantial photoresponses were detected in the presence of only one of the porphyrin species. Fundamental aspects on the dimer structure and photoreactivity were extracted from the photocurrent dependence on the concentration of both porphyrins. Photocurrent spectra as well as analysis of the association constant indicate that the porphyrin species are intimately associated as inner sphere ion pairs. Relevant issues in connection to back electron transfer, heterodimer adsorption, and orientation at the interface are also exposed.

Introduction

Naturally occurring porphyrin dimer plays an essential role in photosynthetic centers in bacteria such as *Rhodospseudomonas viridis*.^{1,2} The *special pair* of bacteriochlorophylls exhibits efficient charge transfer to quinone species within a fraction of a nanosecond. Extensive research on the homogeneous photochemistry and photophysics has been carried out mainly in covalently linked porphyrin resembling the structure of the *special pair*.^{3,4} An alternative type of dimer can be formed by spontaneous association of cationic and anionic porphyrin species as reported by Linschitz et al.^{5–7} Flash photolysis and time-resolved EPR spectroscopy of the pair zinc meso-tetrakis-[4-trimethylanilinium] porphyrin (ZnTTAP) and copper meso-tetrakis(*p*-sulfonatophenyl) porphyrin (CuTPPS) suggested the formation of localized triplet states upon illumination, featuring lifetime of 30 μ s in water/acetone mixtures.⁷ It has also been considered that a small fraction of the dimer species exhibits the appropriate porphyrin orientation for electron transfer involving a singlet precursor.⁷

The interfacial reactivity of this type of dimer is largely unknown. Recently, D'Souza and co-workers have shown that cobalt tetrakis(*N*-methylpyridyl)porphyrin (CoTMPyP) and CoTPPS also form ion pairs with catalytic properties toward

the four-electron reduction of oxygen.⁸ The heterodimer species were adsorbed on glassy carbon electrodes. Interestingly, the pair involving CoTMPyP and the free ligand H₂TPPS showed catalytic properties only for the two-electron mechanism.⁸ In a previous contribution, we have introduced photocurrent responses at the polarized water/1,2-dichloroethane (DCE) interface featuring the heterodimer ZnTPPS–ZnTMPyP.⁹ Under similar conditions, this heterodimer exhibits photocurrent responses up to 50 times larger than those observed for the anionic zinc tetrakis(carboxyphenyl) porphyrin (ZnTPPC).^{10–12} In the present manuscript, the nature of these photoresponses is examined in the presence of the hydrophobic quenchers decamethylferrocene (DCMFC) and tetracyanoquinodimethane (TCNQ). The photocurrent dependence on the concentration of each of the porphyrin species suggests that the association process occurs in solution followed by adsorption of the porphyrin pair at the liquid/liquid junction.

Experimental Section

The electrochemical cell employed for all experiments is represented in Figure 1. The organic phase supporting electrolyte was bis(triphenylphosphoranylidene) ammonium tetrakis (4-chlorophenyl) borate (BTTPATPBCl). Details on the electrolyte preparation and photoelectrochemical set up have been given previously.^{9–12} The surface area of the liquid/liquid junction was 1.53 cm². Illumination was provided by a green He–Ne laser (543 nm) or by a 450 W arc-Xe lamp in conjunction with a grating monochromator. Sodium tetrakis-

(1) Deisenhofer, J.; Epp, O.; Miki, K.; Huber, R.; Michel, H. *Nature* **1985**, 618.

(2) Chabron, J.-C.; Chardon-Noblat, S.; Harriman, A.; Heitz, V.; Sauvage, J.-P. *Pure Appl. Chem.* **1993**, 65, 2343–2349.

(3) Kalyanasundaram, K. *Photochemistry of Polypyridine and Porphyrin Complexes*; Academic Press: London, 1992.

(4) Balzani, V.; Scandola, F. *Supramolecular Photochemistry*; Horwood: Chichester, 1991.

(5) Ojadi, E.; Selzer, R.; Linschitz, H. *J. Am. Chem. Soc.* **1985**, 107, 7783–7784.

(6) van Willigen, H.; Das, U.; Ojadi, E.; Linschitz, H. *J. Am. Chem. Soc.* **1985**, 107, 7784–7785.

(7) Hugerat, M.; Levanon, H.; Ojadi, E.; Biczok, L.; Linschitz, H. *Chem. Phys. Lett.* **1991**, 181, 400–406.

(8) D'souza, F.; Hsieh, Y. Y.; Deviprasad, G. R. *Chem. Commun.* **1998**, 1027–1028.

(9) Fermín, D. J.; Duong, H.; Ding, Z.; Brevet, P.-F.; Girault, H. H. *Electrochem. Commun.* **1999**, 1, 29–32.

(10) Fermín, D. J.; Ding, Z.; Duong, H. D.; Brevet, P. F.; Girault, H. H. *J. Chem. Soc., Chem. Commun.* **1998**, 1125–1126.

(11) Fermín, D. J.; Ding, Z.; Duong, H.; Brevet, P.-F.; Girault, H. H. *J. Phys. Chem. B* **1998**, 102, 10334–10341.

(12) Fermín, D. J.; Duong, H.; Ding, Z.; Brevet, P.-F.; Girault, H. H. *Phys. Chem. Chem. Phys.* **1999**, 1, 1461–1467.

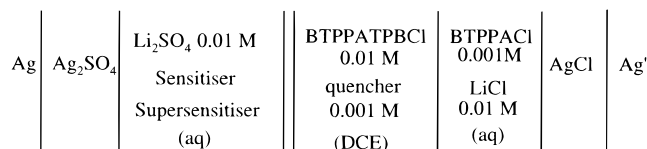
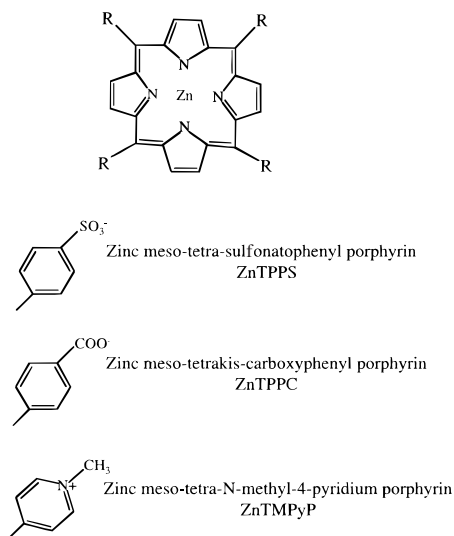


Figure 1. Schematic representation of the electrochemical cell. BTTPATPBCl stands for bis(triphenyl-phosphoranylidene) ammonium tetrakis (4-chlorophenyl) borate.

Scheme 1. Water Soluble Porphyrin Species Employed as Sensitizers at the Water |DCE Interface^a



^a The group R in the meso position corresponds to the functional groups shown.

(carboxyphenyl) zinc porphyrin, sodium *meso*-tetra-sulfonatophenyl zinc porphyrin and *meso*-tetra-*N*-methyl-4-pyridium zinc porphyrin tosylate were purchased from Porphyrin Inc. The structures of these porphyrin species are displayed in Scheme 1. All Galvani potential differences were estimated by taking the formal potential of the standard ions tetramethylammonium and tetrapropylammonium as $\Delta_o^w \phi_{TMA}^{\circ} = 0.160$ V and $= \Delta_o^w \phi_{TPA}^{\circ} + 0.093$ V.¹³

Results and Discussions

Transfer Potential of the Porphyrins ZnTPPS and ZnTMPyP. In the cell represented in Figure 1, the ionic porphyrin species are initially present in the aqueous phase. Upon polarization across the liquid/liquid junction, these porphyrins can be transferred from water to DCE. The formal transfer potential for each of the ionic species is not only determined by their charge but also by the difference in solvation energy in both phases.¹⁴ The solubility of the porphyrins ZnTPPS⁴⁻, ZnTPPC⁴⁻, and ZnTMPyP⁴⁺ is rather negligible in DCE. In Figure 2a, the voltammetric responses associated with the transfer of ZnTPPS⁴⁻ exhibit rather sharp features as a function of the scan rate. By convention, transfer of a negative charges from water to the organic phase is associated with negative currents. The separation between the transfer peaks at slow scan rates approaches the expected 15 mV for a tetravalent anion. The position of the transfer response establishes a formal transfer potential of $\Delta_o^w \phi_{ZnTPPS}^{\circ} = -0.22 \pm 0.01$ V. At slow potential sweep rates, it is also observed that the positive peak is followed by a second smaller response at about -0.150 V.

(13) Shao, Y. Ph.D. Thesis, University of Edinburgh: Edinburgh, 1991.
(14) Girault, H. H. In *Modern Aspects of Electrochemistry*; Bockris, J. O. M., Conway, B. E., White, R. E., Eds.; Plenum Press: New York, 1993; pp 1–62.

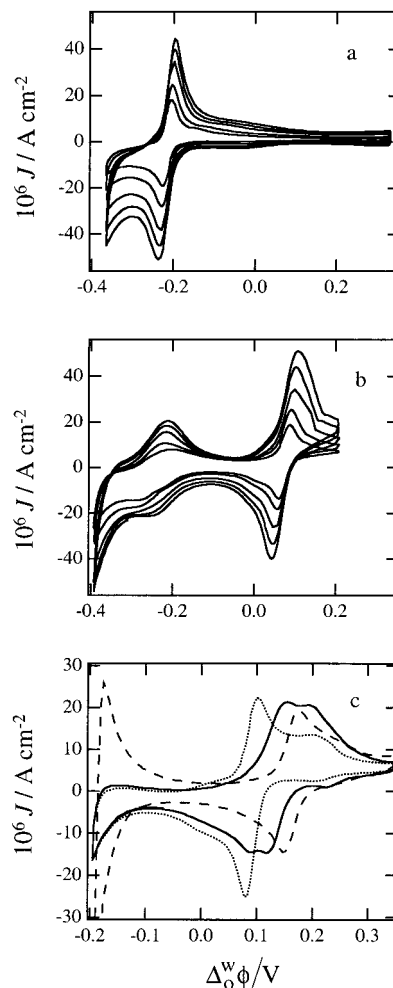


Figure 2. Cyclic voltammograms obtained in the dark for 5×10^{-6} mol dm⁻³ ZnTPPS (a) and 5×10^{-6} mol dm⁻³ ZnTMPyP (b) at 10, 20, 40, 60, and 80 mV s⁻¹. No quencher species was introduced in the organic phase. Transfer responses associated with 5×10^{-6} mol dm⁻³ ZnTMPyP (c) in the presence of 5×10^{-7} mol dm⁻³ ZnTPPS (···), 5×10^{-6} mol dm⁻³ ZnTPPS (—), and 5×10^{-5} mol dm⁻³ ZnTPPS (---) at 20 mV s⁻¹.

The magnitude of this response increases with increasing scan rate, extending over a potential range of more than 200 mV at 80 mV s⁻¹. This voltammetric signal is related to the adsorption of the porphyrin species at the liquid/liquid junction. Adsorption of ZnTPPS⁴⁻ has been confirmed by differential capacitance measurements. For a concentration of 5×10^{-5} mol dm⁻³, the potential of minimum capacitance is shifted by 75 mV toward positive potentials with respect to the value obtained for the same interface in the absence of the porphyrin species, (10 ± 5 mV). The shift in the potential of zero charge is approximately 3 times smaller than that observed for the porphyrin ZnTPPC⁴⁻ under similar conditions.¹¹

Rather complicated voltammograms were also obtained in the presence of ZnTMPyP⁴⁺ as displayed in Figure 2b. Two responses are clearly observed within the potential window. The response at negative potentials corresponds to the transfer of tosylate present as counterion of the cationic porphyrin. Cyclic voltammograms in the presence of sodium tosylate show a similar response with a formal transfer potential $\Delta_o^w \phi_{\text{tosylate}}^{\circ} = -0.28 \pm 0.01$ V. At more positive potentials, the transfer of ZnTMPyP⁴⁺ is observed featuring the convolution of two or more responses in a narrow potential range. At 10 mV s⁻¹, a peak to peak separation of about 15 mV is observed, providing a formal transfer potential of $\Delta_o^w \phi_{ZnTMPyP}^{\circ} = 0.05 \pm 0.03$ V.

As the scan rate is increased, postpeak features are also developed. Transposing the analysis developed by Wopschall and Shain for redox processes involving adsorbed species,¹⁵ the presence of postpeak responses is connected to strongly adsorbed reactant species. In this sense, these voltammetric features may suggest that the transfer of ZnTMPyP⁴⁺ is also preceded by an adsorption step. Contrary to the cases of ZnTPPC⁴⁻ and ZnTPPS⁴⁻ studies of the excess charge associated with the porphyrin adsorption by impedance measurements are rather complex due to the proximity of the transfer potential range. On the other hand, preliminary studies by potential modulated fluorescence spectroscopy and optical surface second harmonic generation in total internal reflection from the organic phase suggest the presence of adsorbed ZnTMPyP⁴⁺ at potentials more negative than the formal transfer potential.

The evolution of the transfer response associated with ZnTMPyP⁴⁺ with increasing concentrations of ZnTPPS⁴⁻ is also shown in Figure 2c. As the concentration of the anionic porphyrin is increased, the transfer of ZnTMPyP⁴⁺ effectively shifts toward more positive potentials. The shape of the response is also affected, revealing new features at either side of the transfer signal. This interesting behavior suggests an association equilibrium involving both porphyrins in the aqueous phase. Considering the Nernst equation for the ZnTMPyP⁴⁺ transfer

$$\Delta_o^w \phi = \Delta_o^w \phi_{\text{ZnTMPyP}^{4+}}^{\circ'} + \frac{RT}{4F} \ln \left(\frac{[\text{ZnTMPyP}]_o}{[\text{ZnTMPyP}]_w} \right) \quad (1)$$

and the association constant of both porphyrins in aqueous phase K_C

$$K_C = \frac{[\text{dimer}]_w}{[\text{ZnTMPyP}]_w [\text{ZnTPPS}]_w} \quad (2)$$

it follows that the shift of the formal transfer potential of ZnTMPyP for a given concentration of ZnTPPS corresponds to

$$\Delta_o^w \phi_{\text{ZnTMPyP}^{4+} + \text{ZnTPPS}^{4-}}^{\circ'} - \Delta_o^w \phi_{\text{ZnTMPyP}^{4+}}^{\circ'} = \frac{RT}{4F} \ln(K_C [\text{ZnTPPS}]_w) \quad (3)$$

Considering the shift of the transfer signal as a function of the ZnTPPS concentration in Figure 2c, the association constant can be estimated as $(3.0 \pm 2.5) \times 10^7 \text{ mol}^{-1} \text{ dm}^3$. Unfortunately, the complexity of the transfer signal introduces considerable uncertainties in the determination of the transfer potentials. Interestingly, association constants of the same magnitude have been reported for several porphyrin ion pairs in water/acetone mixtures at room temperature.⁵ As shown in the next section, photocurrent dependence on the concentration of both porphyrins does confirm these results. The voltammetric responses in Figure 2c also illustrate the polarization window where heterogeneous photoinduced electron-transfer responses can be studied without significant perturbations arising from the transfer of porphyrin species. From this figure, the potential window extends over $\sim 300 \text{ mV}$. Furthermore, no additional features were observed in the presence of organic phase quenchers, indicating that the ground state of the sensitizer is not involved in any electron-transfer processes within the polarization window.

Photocurrent Responses Involving the Heterocomplex ZnTPPS–ZnTMPyP. Photocurrent transient responses in the

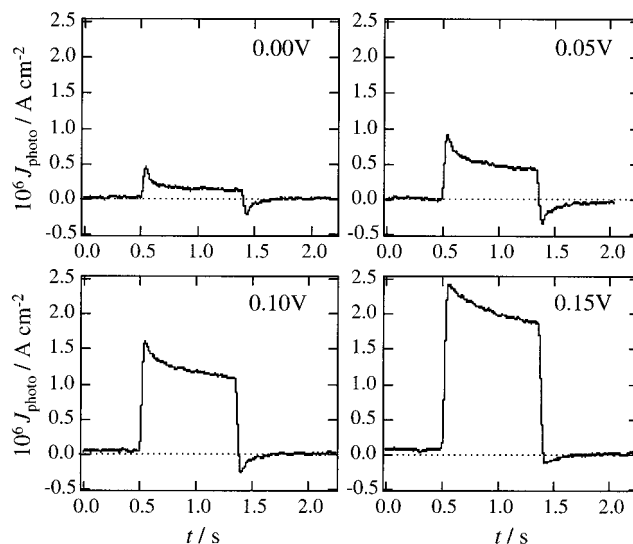


Figure 3. Photocurrent transients originating from the photooxidation of DCMFc in the presence of $5 \times 10^{-5} \text{ mol dm}^{-3}$ ZnTPPS and ZnTMPyP at various Galvani potential differences. Photon flux was $6.4 \times 10^{15} \text{ cm}^{-2} \text{ s}^{-1}$ at 543 nm.

presence of equimolar concentrations of ZnTPPS⁴⁻ and ZnTMPyP⁴⁺ in the aqueous phase and the electron donor decamethylferrocene (DCMFc) in DCE are displayed in Figure 3. It is observed that the photocurrent increases as the applied Galvani potential increases. These results resemble the behavior observed for the heterogeneous quenching of ZnTPPC by ferrocene derivatives.^{11,12} Negligible photoresponses are observed in the absence of the organic phase quencher. Interestingly, no substantial photocurrent is detected in the presence of only one of the porphyrin species at the same experimental conditions. This is a surprising result as both porphyrins exhibit rather positive redox potentials in the excited state ($E_{\text{ox}}^* > 1 \text{ V}$). From this behavior, it is evident that the photoactive species corresponds to a heterostructure involving ZnTPPS⁴⁻ and ZnTMPyP⁴⁺.

The overall photoresponses in Figure 3 are substantially higher at potentials close to 0 V in comparison to the monomer ZnTPPC⁴⁻. For instance, at 0.10 V the photocurrent in the presence of ZnTPPS⁴⁻ and ZnTMPyP⁴⁺ is approximately 40 times larger than in the case of ZnTPPC for the same photon flux.¹¹ Another relevant observation is related to the fact that no enhancement of the photocurrent occurred in the presence of the pair ZnTPPC–ZnTMPyP. Preliminary flash photolysis studies do reveal quenching of the triplet lifetime for the pair ZnTPPC–ZnTMPyP, indicating an effective interaction between both monomers in solution. However, photocurrent responses associated with the quenching of ZnTPPC are very little affected by the presence of ZnTMPyP. As discussed in the next section, the differences in the heterogeneous photochemistry between ZnTPPS–ZnTMPyP and ZnTPPC–ZnTMPyP are connected to the adsorption behavior of these porphyrins at the water/DCE interface.

The features of the photocurrent transients in Figure 3, even at potentials close to the edge of the polarizable window, are consistent with a heterogeneous electron-transfer mechanism. Effectively, the “instantaneous” photocurrent observed upon illumination is proportional to the flux of electron injection to the heterocomplex excited state.^{11,12} The flux of electron injection is dependent on the (i) interfacial concentration of the reactants, (ii) the photon flux to the interface, (iii) the optical capture cross section of the sensitizer, and (iv) the competition

(15) Bard, A. J.; Faulkner, L. R. *Electrochemical Methods*; Wiley: New York, 1980.

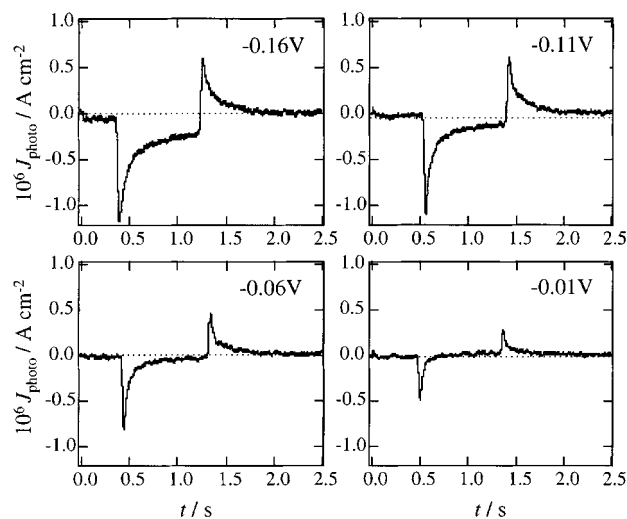


Figure 4. Photocurrent transients obtained in the presence of 5×10^{-5} mol dm $^{-3}$ ZnTPPS and ZnTMPyP in the aqueous phase, and TCNQ as the organic phase quencher. Negative photocurrents are associated with the photoreduction of TCNQ. The positive overshoot in the off transient is linked to back electron transfer to the oxidized ground state sensitizer. Photon flux was 6.4×10^{15} cm $^{-2}$ s $^{-1}$ at 543 nm.

between electron transfer and decay of the excited state.¹¹ In the case of ionic porphyrin ZnTPPC $^{4-}$, both the coverage of the sensitizer at the liquid/liquid interface as well as the phenomenological photoinduced electron-transfer rate constant have been found to be dependent on the Galvani potential difference.^{11,12} Mechanisms involving homogeneous quenching followed by transfer of charged products can be effectively excluded from this analysis as these processes feature essentially zero initial photocurrent and slow rising photoresponses in the time scale of $1-10^2$ s.¹⁶⁻¹⁸

The relaxation observed following the initial photocurrent and the negative overshoot during the off transient are related to back electron-transfer processes.^{11,12} Recombination is rather dependent on the redox properties of the organic species. In Figure 4, photocurrent strongly decreases after the initial response in the presence of the electron acceptor TCNQ. In this case, the photoinduced electron-transfer involves negative photocurrents as the electron injection occurs from the porphyrin heterodimer to TCNQ. It is also observed that the negative photocurrent increases as the potential is shifted toward the negative edge of the window. The positive overshoot in the off-transient reflects a back electron transfer to the oxidized ground state sensitizer. The competition between product separation and recombination is not only dependent on the Galvani potential difference,¹² but it could also be affected by interaction with supersensitizers.⁹ A schematic representation of the overall mechanism, including the supersensitization step, is shown in Figure 5a. It is envisaged that the recombination step is in competition with electron exchange between the photoinduced intermediate species and the supersensitizer located in the aqueous phase. In a previous report, it was demonstrated that the photocurrent relaxation in Figure 4 is partially suppressed in the presence of an equimolar concentration of the hexacyanoferrate couple acting as supersensitizer.⁹

(16) Kotov, N. A.; Kuzmin, M. G. *J. Electroanal. Chem.* **1990**, 285, 223.

(17) Kotov, N. A.; Kuzmin, M. G. *J. Electroanal. Chem.* **1992**, 341, 47-60.

(18) Kotov, N. A.; Kuzmin, M. G. *J. Electroanal. Chem.* **1992**, 338, 99.

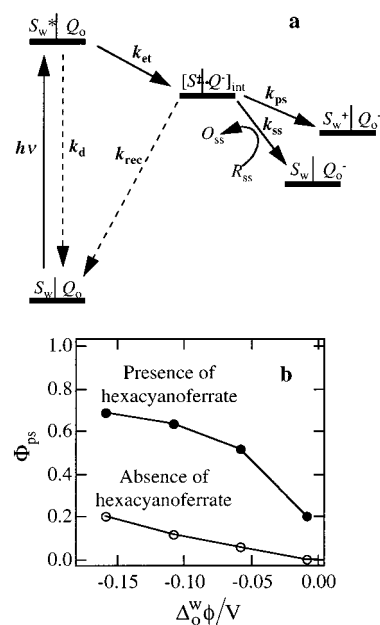


Figure 5. Schematic representation of a photoinduced electron transfer from an aqueous soluble sensitizer (S_w) to an organic phase electron acceptor (Q_o) featuring a redox couple acting (R_{ss}/O_{ss}) as a supersensitizer (a). The rate constants k_{et} , k_d , k_{ps} , k_{rec} , and k_{ss} stand for electron transfer, decay of the excited state, product separation, back-electron transfer and supersensitization respectively. Product separation efficiency for the photoreduction of TCNQ as a function of the Galvani potential difference in the presence and absence of an equimolar ratio (2.5×10^{-4} mol dm $^{-3}$) of the hexacyanoferrate redox couple (b). Other experimental parameters as in Figure 4.

The product separation efficiency (Φ_{ps}) can be defined as the ratio between the steady state (J_{ss}) and initial photocurrent (J_0)

$$\Phi_{ps} = J_{ss}/J_0 \quad (4)$$

The effect of the Galvani potential difference and the supersensitizer $[\text{Fe}(\text{CN})_6]^{4-}/[\text{Fe}(\text{CN})_6]^{3-}$ on the product separation efficiency is contrasted in Figure 5b. It is observed that the efficiency increases from ~ 0.2 to 0.7 at -0.15 V upon adding 2.5×10^{-4} mol dm $^{-3}$ of the hexacyanoferrate redox couple. This effect clearly indicates that the photocurrent decay and overshoot are indeed connected to a heterogeneous electron-transfer process. Despite the noticeable increase of the steady-state photocurrent in the presence of the supersensitizer, a considerable fraction of the photoinduced intermediate species still undergoes back electron transfer. Consequently, Φ_{ps} is also dependent on the Galvani potential difference under these conditions. Analysis of the potential dependence of the electron transfer and recombination rate constant for the monomer ZnTPPC $^{4-}$ has suggested that both processes involve an activated step which is related to redox and interfacial properties of the quencher species.¹²

Interfacial Behavior of the Pair ZnTPPS–ZnTMPyP.

Although the previous analysis indicates that the photoactive species involves both zinc porphyrins, the nature of this heterocomplex should be addressed in more detail. In Figure 6, photocurrent spectra recorded at various potentials are compared to the absorption features of the free monomers ZnTPPS and ZnTMPyP in solution. In these experiments, the relative input photon flux was monitored by a photomultiplier tube connected to a liquid light guide. Subsequently, photocurrent responses were normalized to the output of the photomultiplier tube at

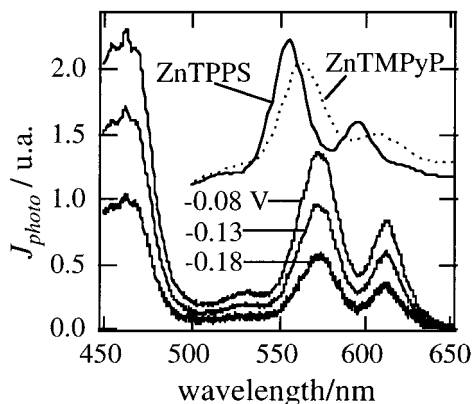


Figure 6. Photocurrent spectra associated with the photooxidation of DCMFc by the heterodimer ZnTPPS–ZnTMPyP. Photocurrent responses were normalized to the input flux of photon at each wavelength. Absorption features for the free monomer ZnTPPS and ZnTMPyP in aqueous solution are also superimposed.

each wavelength.¹⁰ It is observed that the photocurrent responses associated with the Q-band transitions are red-shifted respect to the absorption signal of the free porphyrin monomers. This behavior is rather different to the observed for ZnTPPC, in which photocurrent and absorption maxima coincide within the same wavelength range.¹⁰ As mentioned previously, photocurrent responses arising from the free monomers ZnTPPS and ZnTMPyP⁴⁺ are negligible, therefore the photocurrent spectra in Figure 6 reflect only the absorption behavior of the heterodimer species. The red shift of the Q-band suggests that the dimer ZnTPPS–ZnTMPyP forms an inner-sphere ion pair.¹⁹ Other porphyrin pairs have also shown similar spectroscopic behavior.⁵ In this type of ion pair, both species are in close proximity losing the first solvation shell. In addition, inner-sphere ion pairs can be regarded as dipolar polyatomic ions with nonspherical charge distribution.²⁰ In the case of ZnTMPyP–ZnTPPS, the overall charge of the pair structure is zero.

The adsorption of the porphyrin heterocomplex at the water/DCE interface can be followed by the concentration dependence of the photocurrent signal. Photocurrent potential curves obtained under chopped illumination at 12 Hz and lock-in detection at various concentration of ZnTPPS and ZnTMPyP are displayed in Figure 7. The real component of the photocurrent in the presence of DCMFc was considerably larger than the quadrature component, indicating that transient responses associated with recombination and interfacial charging current are rather negligible at this frequency.¹² The potential dependence of the real part of the photocurrent reflects increasing photocurrent with increasing Galvani potential difference as illustrated in Figure 3. A rather interesting behavior is also observed from the photocurrent dependence on the monomer concentration. The increase of the photocurrent with increasing concentration of ZnTPPS and ZnTMPyP seems rather similar at all Galvani potential differences. This trend is more clearly displayed in Figure 8, where photocurrent isotherms are plotted at various potentials. As a first approximation, this effect can be rationalized in terms of the association of both porphyrin species in solution leading to electrically neutral photoactive species. The photocurrent responses are effectively linked to adsorbed heterodimer species which are in equilibrium with the total concentration in solution. Due to the absence of a net charge

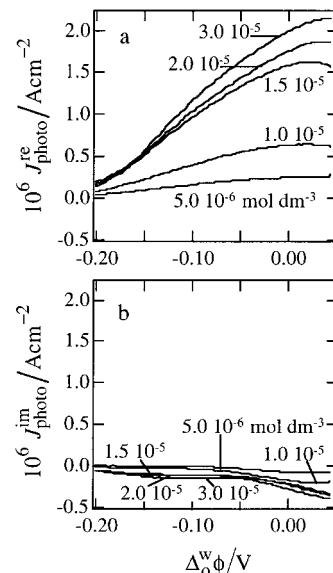


Figure 7. Real (a) and imaginary (b) component of the photocurrent in the presence of DCMFc and various concentration of ZnTPPS and ZnTMPyP. The light chopping frequency was 12 Hz. The photon flux was $6.4 \times 10^{15} \text{ cm}^{-2} \text{ s}^{-1}$. It is observed that the imaginary part of the photocurrent is negligible with respect to the real part, indicating that the photoresponses are effectively in phase at this frequency.

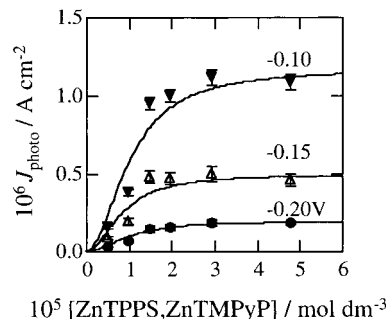


Figure 8. Photocurrent dependence on the concentration of ZnTPPS and ZnTMPyP at various Galvani potential differences. Experimental conditions as in Figure 7.

on the heterodimer species, the adsorption equilibrium remains largely independent of the Galvani potential difference. Consequently, from the phenomenological mechanism introduced in previous work,^{11,12} the photocurrent response in the absence of recombination is expressed as

$$j_{\text{photo}} = j_{\text{photo}}^{\text{max}} \left[\frac{\beta[\text{dimer}]_{\text{w}}}{1 + \beta[\text{dimer}]_{\text{w}}} \right] \quad (5)$$

where $j_{\text{photo}}^{\text{max}}$ is the photocurrent corresponding to a full compact monolayer of the dimer species

$$j_{\text{photo}}^{\text{max}} = e \frac{k_{\text{et}}}{k_{\text{et}} + k_{\text{d}}} I_0 \sigma N_{\text{s}} \quad (6)$$

e is the electronic charge, k_{et} the pseudo-first-order rate constant for electron transfer, k_{d} the rate constant of excited state relaxation, I_0 the photon flux, σ the capture cross section, and N_{s} the surface density of dimer species in a close compact monolayer. Equations 5 and 6 are associated with a mechanism where photoresponses are determined by a competition between relaxation of the excited state and electron transfer. The parameter β corresponds to the Langmuir isotherm parameter. The concentration of the dimer in solution is simply given by

(19) Nancollas, G. H. *Interactions in electrolyte solutions*; Elsevier: Amsterdam, The Netherlands, 1966.

(20) Marcus, Y. *Ion solvation*; John Wiley and Sons Ltd.: Chichester, 1985.

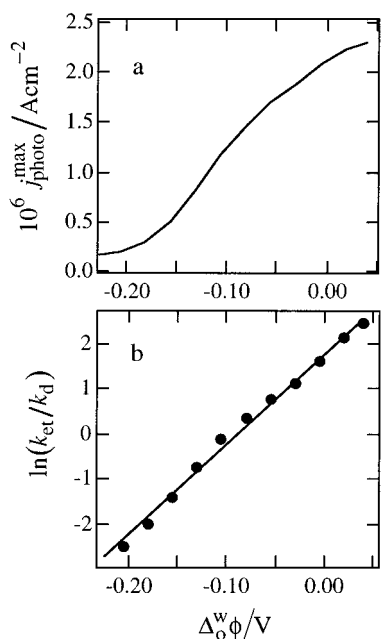


Figure 9. Potential dependence of the photocurrent associated with a full monolayer of porphyrin heterodimer (a) obtained from the fittings of the photocurrent isotherms (Figure 8). The ratio of the pseudo-first-order electron transfer and decay of the excited rate constants as a function of the Galvani potential difference (b) was estimated from eq 7, assuming $2.5 \times 10^{14} \text{ cm}^{-2}$ as the maximum surface density of dimer species. Considering a Butler–Volmer dependence of k_{et} , a transfer coefficient of 0.5 is estimated.

the association equilibrium for the two porphyrin monomers as defined in eq 2.

The dependence of the photocurrent on the concentration of ZnTPPS and ZnTMPyP at various Galvani potential differences is displayed in Figure 8. Fittings employing eq 5 are also shown as continuous lines. Three parameters were adjusted for each Galvani potential difference, $j_{\text{photo}}^{\text{max}}$, K_{C} and β . The parameters K_{C} and β were found almost independent of the applied potential. For instance, the association constant K_{C} exhibited an average value of $(6 \pm 1) \times 10^7 \text{ mol}^{-1} \text{ dm}^3$ throughout the potential range. This value is comparable to the preliminary estimations based on the shift of the ZnTMPyP transfer potential in the presence of ZnTPPS (cf. Figure 2). In turn, the increase of the photocurrent with increasing potential is associated with the parameter $j_{\text{photo}}^{\text{max}}$. The potential dependence of $j_{\text{photo}}^{\text{max}}$ is displayed in Figure 9a. This behavior reflects an increase of the electron-transfer rate with respect to the relaxation of the excited state. Another interesting aspect arising from this analysis is the rather high values obtained for $j_{\text{photo}}^{\text{max}}$ in comparison to the responses observed for the monomer ZnTPPC.¹¹ Taking a capture cross section of 10^{-17} cm^2 at 543 nm for the heterodimer, the photocurrent density is 4–5 times higher than the value expected for a close packed layer of porphyrin molecules lying coplanar to the interface.¹¹ Assuming that photocurrent arises from the first monolayer of adsorbed porphyrin species, the high values of $j_{\text{photo}}^{\text{max}}$ can be taken as an evidence for a specific orientation of the adsorbed porphyrin pairs at the interface. On the basis that porphyrin heterodimer consists of an electrically neutral dipolar molecule, it could be envisaged a kind of self-assembling mechanism for the adsorption process at the liquid/liquid junction. The interfacial orientation of heterodimer species may also play a fundamental role on the kinetics of photoinduced electron transfer.

A closer look into the potential dependence of $j_{\text{photo}}^{\text{max}}$ revealed that the increment of k_{et} with increasing potential approaches a Tafel behavior. The ratio $k_{\text{et}}/k_{\text{d}}$ can be estimated by rearranging eq 6

$$k_{\text{et}}/k_{\text{d}} = \frac{1}{(eI_0\sigma N_s/j_{\text{photo}}^{\text{max}}) - 1} \quad (7)$$

In Figure 9b, this ratio is plotted as a function of the Galvani potential difference assuming a value of N_s of $2.5 \times 10^{14} \text{ cm}^{-2}$. The exponential increment of $k_{\text{et}}/k_{\text{d}}$ with increasing Galvani potential can be described in terms of a Tafel relation with a transfer coefficient close to $\alpha = 0.5$. These results have been phenomenologically interpreted in terms of an activation barrier for the electron-transfer process.^{11,12} In addition, taking the lifetime of the triplet state as 30 μs after the report by Hugerat et al.⁷ for a similar porphyrin ion pair, k_{et} may lie in the range of 10^4 – 10^5 s^{-1} . The value of k_{et} is within the same order of magnitude to the estimated for the monomer ZnTPPC. Consequently, these results seem to indicate that the larger photocurrent observed for the pair ZnTPPS–ZnTMPyP in comparison to the porphyrin ZnTPPC is mostly connected to a higher interfacial concentration of the porphyrin ion pair.

The value of k_{et} , as extracted from the previous analysis, corresponds to the integral of the electron-transfer rate over the distance separating the adsorbed sensitizer and the organic redox couple.¹¹ Recent descriptions of the interfacial structure of ITIES based upon lattice-gas approximation²¹ and molecular dynamics²² suggest that the interfacial region between water and DCE extends over an average distance of 1 nm. Taking this value as a first approximation, the pseudo-first-order heterogeneous rate constant is of the order of $10^{-2} \text{ cm s}^{-1}$. Although this magnitude is ~ 10 times faster than previously reported rate constants for heterogeneous electron transfer at ITIES in the dark,^{23–27} it is still 2–3 orders of magnitude slower than the upper limit for outer sphere adiabatic electron-transfer reactions from the Marcus' model.^{28–30}

According to the values obtained for β , the Gibbs energy of adsorption (ΔG_{ads}) can be estimated as $-22.8 \pm 0.4 \text{ kJ mol}^{-1}$. The magnitude of ΔG_{ads} is approximately half of the value reported for ZnTPPC under similar experimental conditions.^{11,12} This surprising result indicates that, although the adsorption energy for ZnTPPC is larger, a smaller number of these porphyrins can be accommodated at the liquid/liquid junction in comparison to the heterodimer. The large adsorption energy exhibited by ZnTPPC in comparison to ZnTPPS is also responsible for the difference in photoreactivity of the corresponding dimer structures. As mentioned earlier, no enhancement of the photocurrent associated with the quenching of ZnTPPC is observed upon addition of the cationic ZnTMPyP. Although spectroscopic evidence suggests the formation of ion pairs between ZnTPPC and ZnTMPyP in solution, the adsorption sites at the interface are expected to be mostly occupied

(21) Schmickler, W. *J. Electroanal. Chem.* **1997**, 429, 123–127.

(22) Benjamin, I. *Annu. Rev. Phys. Chem.* **1997**, 48, 407.

(23) Cheng, Y.; Schiffrin, D. J. *J. Chem. Soc., Faraday Trans.* **1993**, 89, 199–205.

(24) Ding, Z.; Fermín, D. J.; Brevet, P.-F.; Girault, H. H. *J. Electroanal. Chem.* **1998**, 458, 139–148.

(25) Tsionsky, M.; Bard, A. J.; Mirkin, M. V. *J. Phys. Chem.* **1996**, 100, 17881–17888.

(26) Tsionsky, M.; Bard, A. J.; Mirkin, M. V. *J. Am. Chem. Soc.* **1997**, 119, 10785–10792.

(27) Shi, C.; Anson, F. C. *J. Phys. Chem. B* **1999**, 103, 6283–6289.

(28) Marcus, R. A. *J. Phys. Chem.* **1990**, 94, 4152–5.

(29) Marcus, R. A. *J. Phys. Chem.* **1990**, 94, 1050–5.

(30) Marcus, R. A. *J. Phys. Chem.* **1991**, 95, 2010–13.

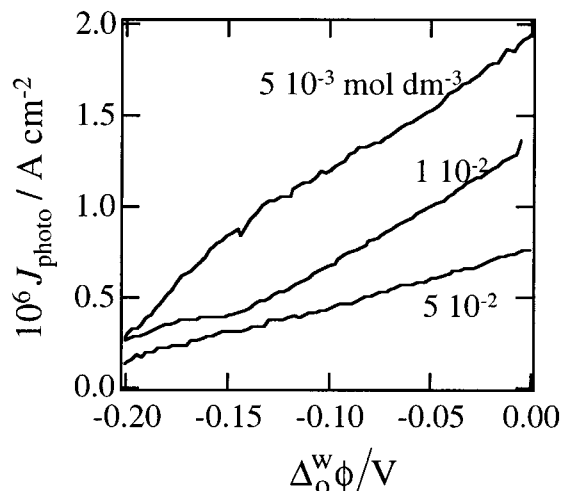


Figure 10. Photocurrent potential curves in the presence of 5×10^{-5} mol dm^{-3} of ZnTPPS and ZnTMPyP, and DCMFc as quencher at various concentration of Li_2SO_4 . Other experimental conditions as in Figure 7. Photocurrent responses were effectively in-phase throughout the potential range for all concentrations of the aqueous supporting electrolyte.

by the anionic porphyrin instead of the dimer species. This behavior shows that the interfacial photoreactivity of ion pair dimers not only depends on the association of the porphyrin species, but also on the adsorption properties of each of the species involved.

Dependence of Photoresponses on the Ionic Strength of the Aqueous Phase. Photocurrent responses for a concentration of 5×10^{-5} mol dm^{-3} of the porphyrins ZnTPPS and ZnTMPyP are displayed in Figure 10 for various concentrations of Li_2SO_4 . It is observed that the overall photocurrent decreases with increasing concentration of the supporting electrolyte. Similar to the results in Figure 7, the imaginary component of the photocurrent was negligible in comparison to the real component. Photocurrent isotherm analysis revealed that the ΔG_{ads} and K_C are dependent on the supporting electrolyte concentration. Figure 11 shows that ΔG_{ads} becomes more negative, and K_C decreases with increasing concentration of Li_2SO_4 . The origin of the ΔG_{ads} dependence on the aqueous ionic strength is yet to be rationalized. In principle, the increase of the supporting electrolyte concentration may involve higher screening of the local charge associated with the porphyrin units, enhancing the surface assembling of adsorbed dimer species.

The behavior of K_C in Figure 11b can be rationalized in terms of a decrease in the activity coefficient of the charged porphyrin monomers with increasing concentration of the supporting electrolyte. To quantify this effect, the association constant involving the activities of the ionic species (K_A) can be expressed as

$$K_A = \frac{a_{\text{dimer}}}{(a_{\text{ZnTPPY}^{4-}})(a_{\text{ZnTMPyP}^{4+}})} = \frac{K_C}{(\gamma_{\text{ZnTPPS}^{4-}})(\gamma_{\text{ZnTMPyP}^{4+}})} \quad (8)$$

where the activity coefficient of the heterodimer is assumed independent of the supporting electrolyte concentration and close to unity. Activity coefficients of highly charged species as a function of the ionic strength (I) have been described by the formula proposed by Davies in 1938¹⁹

$$-\log \gamma_z = Az^2 \left(\frac{I^{1/2}}{1 + I^{1/2}} - CI \right) \quad (9)$$

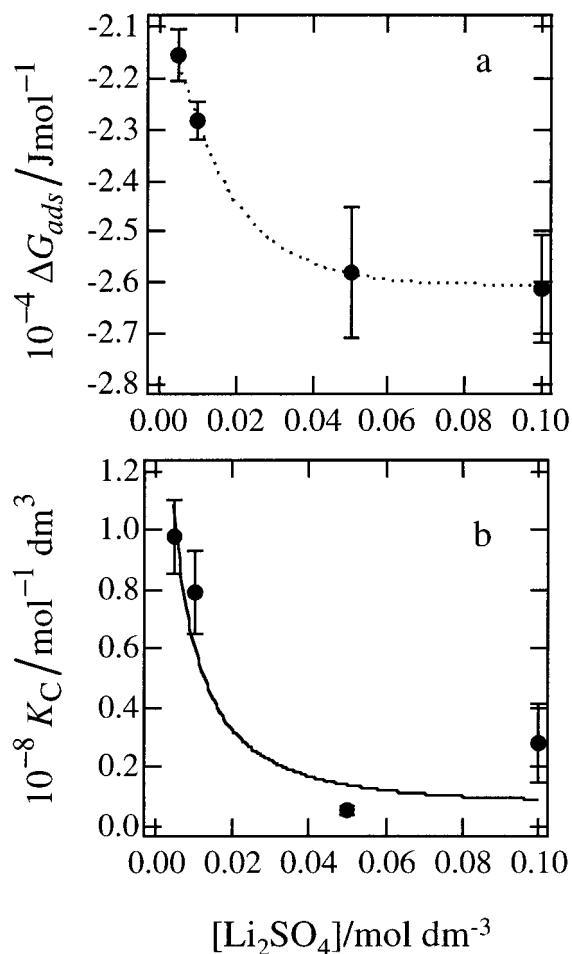


Figure 11. Dependence of the Gibbs energy of adsorption (a) and ZnTPPS–ZnTMPyP association constant (b) as function of the aqueous supporting electrolyte concentration. Both parameters were obtained from photocurrent isotherms as exemplified in Figure 8.

where A is the constant derived from the Debye–Hückel theory, i.e., 0.509 for aqueous solution at 25 °C, and C is an adjusting parameter. Analysis of a large range of electrolytes have provided values for C between 0.2 and 0.4 kg mol^{-1} .¹⁹ The solid line in Figure 11b corresponds to a fit based on eqs 8 and 9, assuming a value of 0.3 kg mol^{-1} for C . This result effectively confirmed that the K_C dependence on I is associated with changes in the activity coefficients of the charged porphyrins. Nevertheless, it should be mentioned that the previous approximation related to the activity coefficient of the dimer species is not strictly valid in the light of the dependence of ΔG_{ads} on the ionic strength.

It should also be concluded that the decrease in the photocurrent responses with increasing supporting electrolyte concentration (Figure 10) cannot be ascribed only to the dependence of ΔG_{ads} and K_C on the ionic strength. Although the behavior of these two parameters has clear effects on the photocurrent isotherms, the estimated changes in total photocurrent are rather small in comparison to the experimental trend. In turn, the changes in the total photocurrent may reflect changes in the quantum yield, i.e., the ratio between the rates of electron transfer and relaxation of the excited state. It is well-established that the lifetime of the triplet state for several porphyrins decreases with increasing ionic strength of the medium.³ Decreasing photocurrent with increasing supporting electrolyte concentration has also been observed for the monomer ZnTPPC.

Finally, from the value of $K_A = (5.9 \pm 0.8) \times 10^8$ mol⁻¹ dm³, the distance between the ion pair centers (a) can be

estimated employing the expression derived by Fuoss for contact ion pairs²⁰

$$K_A = [(4 \times 10^{-24} \mathbf{N}\pi/3)](a/\text{nm})^3 \exp(b) \quad (10)$$

where \mathbf{N} is the Avogadro's constant and b corresponds to

$$b = |z_{\text{ZnTPPS}}||z_{\text{ZnTMPyP}}|(e^2/4\pi\epsilon_0\mathbf{k})T^{-1}\epsilon^{-1}a^{-1} \quad (11)$$

Evaluation of eqs 10 and 11 provide a contact distance $a = 5.8 \text{ \AA}$. This distance is larger than the interplane separation between the *special pair* of bacteriochlorophyll molecules in the *R. viridis*, i.e., 3.8 \AA .¹ However, in the case of the naturally occurring dimer, the macrocycles are covalently linked. The estimated distance between ZnTPPS and ZnTMPyP, in conjunction with the excitonic effect revealed in the photocurrent spectra (Figure 6) and the apparently noncoplanar adsorption of the heterodimer at the interface point out that the monomeric units are indeed face-to-face oriented. In this respect, this type of heterodimer can be regarded as a spontaneously generated supramolecular structure which not only exhibits similar characteristics to synthetic and naturally occurring dimers, but also is able to self-assemble at the water/DCE interface. The correlation between interfacial orientation of the adsorbed porphyrins and heterogeneous photoreactivity is currently under investigation.

Conclusions

Water soluble anionic ZnTPPS and cationic ZnTMPyP spontaneously associate in solution, generating heterodimer species which undergoes photoinduced heterogeneous electron transfer with hydrophobic redox species at the water/DCE interface. No detectable photocurrent was observed in the presence of only one of the porphyrin species. Photocurrent responses involving the quenchers DCMFc and TCNQ were found dependent on the Galvani potential difference. Strong recombination responses were observed in the presence of the

electron donor TCNQ. In this case, the recombination reaction was partially suppressed by shifting the Galvani potential difference toward more negative values, or by addition of the hexacyanoferrate redox couple acting as supersensitizer.

The photocurrent dependence on the concentration of both porphyrin species suggests that the association processes occur in homogeneous phase, followed by adsorption of the ion pair at the liquid/liquid junction. The adsorption step was effectively independent of the Galvani potential difference, indicating the electrically neutral nature of the ion pair. The Gibbs energy of adsorption and the association constant of the ion pair were also estimated. Although the adsorption energy was found smaller in comparison to the porphyrin ZnTPPC, the photocurrent response under similar condition was found up to 50 times larger for the heterodimer. The difference in the magnitude of the photoresponses mainly arises from a higher surface density in the case of the ZnTPPS–ZnTMPyP ion pair. Experimental evidence suggests that adsorbed heterodimer species are oriented in a noncoplanar fashion with respect to the interface. On the other hand, excitonic effects revealed by photocurrent spectra as well as estimation of the distance separating the pair ZnTPPS–ZnTMPyP indicate the formation of a contact (inner sphere) ion pair. The overall analysis demonstrates that the heterogeneous photoreactivity of sensitizers forming ion pairs is determined not only by the photophysical properties of the supramolecular structure but also by the interfacial behavior of each of the species involved.

Acknowledgment. The authors are grateful for the financial support of the Fonds National Suisse de la Recherche Scientifique project 20-055692.98/1. The enlightening discussions with Riikka Lahtinen from the Helsinki University of Technology are also gratefully acknowledged. Many thanks to Lise Van Long, Carole Claivaz, and Valérie Devaud for their contributions and technical assistance. The Laboratoire d'Electrochimie is part of the European Network ODRELLI (Organization, Dynamics and Reactivity at Electrified liquid/liquid interfaces).

JA992215I